Adaption of Energy Deposition in Helical Drilling of Multidimensional Micro Holes Using Ultrashort Laser Pulses

Chao He[1,2], Dominik Esch[3] and Arnold Gillner[1,2]

[1] *RWTH Aachen University, Chair for Laser Technology LLT, Steinbachstrasse 15, 52074 Aachen, Germany*
E-mail: chao.he@llt.rwth-aachen.de
[2] *Fraunhofer Institute for Laser Technology ILT, Steinbachstrasse 15, 52074 Aachen, Germany*
[3] *Hochschule Bonn-Rhein-Sieg, School of Natural Sciences, Von-Liebig-Strasse 20, 53359 Rheinbach, Germany*

High-precision, multidimensional holes are required in many technical applications. Due to its undercut shape, these kind of holes are usually manufactured from two sides of the work piece including a time-consuming co-axial alignment. Compared to current state of the art, a one-sided drilling strategy has numerous advantages regarding flexibility, precision and process efficiency. In this work, a helical drilling optic and an ultrashort pulse laser are utilized to fabricate a rotationally symmetric multidimensional-shaped hole in one single process step. The influences of single pulse energy, pulse repetition rate, rotation speed of laser beam as well as the drilling time on ablation depth are investigated. By varying the pulse energy and pulse density, the deposited energy per unit length on the single helical path can be adapted and thus the ablation depth can be scaled. With the adapted laser energy deposition, a T-shaped hole with a uniformed depth of about 80 µm inlet is fabricated. Morphological analysis on the hole wall show excellent drilling quality without recast layers or heat-affected zones and roughness Rq < 0.35 µm.

DOI: 10.2961/jlmn.2019.02.0010
Keywords: helical drilling, ultrashort pulse laser, energy deposition, micro processing, multidimensional

1. Introduction

The miniaturization of modern devices needs microstructures such as microholes in the technical components. The mechanical drilling, EDM and chemical etching have been widely applied in the fabrication of such microholes [1,2]. In the last decades, the laser beam drilling has been intensively studied as the laser offers many advantages such as contact-free and thus no tool wear, and high flexibility [3,4]. Nowadays, with the rapid development of ultrashort pulse lasers especially the laser pulse duration in the regime from tens of picosecond down to several hundred of femtoseconds, the dimension of microholes as well as the quality regarding the precision and heat-affected zone (HAZ) can be dramatically improved [4,5]. The ultrashort pulse lasers have been dominantly applied in the fabrication of high-precision microholes, where excellent wall definition and small heat-affected zone are demanded [6–8]. High-precision, multidimensional holes are required in many technical applications such as fuel injectors, de Laval nozzles or micro filters [8–10]. The multidimensional microholes are characterized by a complex profile more than one dimension in the cross-section for instance a converging taper at the hole entrance and a diverging at exit [8]. Due to its undercut shape, these kind of holes are usually manufactured from two sides of the work piece including a time-consuming co-axial alignment [10,11]. To fabricate shaped cooling air holes in a turbine blade, even two laser systems are employed, which makes the preparation work much more complicated and time consuming [12] Compared to current state of the art, a one-sided drilling strategy has numerous advantages regarding flexibility, precision and process efficiency.

The helical drilling optics, which is based on a Dove prism as image rotator, enables the fabrication of a converging-diverging hole within one step [13]. In contrast to a Galvoscanner-based rotating system, the helical path of the laser pulses using helical drilling optics is an analog continuous circle as a result of a total internal reflection of the laser beam passing through the spinning Dove prism, thus, the circularity of the helical path using the helical drilling optics is supreme. In addition, the spatial helical path can be adapted for varied hole profiles by adjusting the optical parameters such as parallel shift and incident angle of laser beam.

In the previous research works, we exhibited the possibility and flexibility in the fabrication of multidimensional rotational symmetric microholes in different materials by using a dynamic helical drilling process [14]. It is evident that the laser energy deposition during the dynamic helical process plays a vital role in shaping the hole profile. In this paper, further systematical studies are carried out to investigate the influences of single pulse energy, pulse repetition rate, rotation speed of laser beam as well as the drilling time on hole profile. The ablation behavior with different parameters

is studied in order to find out an optimized strategy to achieve the fabrication of designated hole profiles.

2. Experimental and methodology

As schematically shown in Fig. 1, a helical drilling system with an ultrashort pulsed laser are utilized to fabricate a rotationally symmetric shaped hole in one single process step. The ultrashort pulse laser source has a pulse duration of about 900 fs, emitting an average power of 75 watts at a wavelength of 515 nm and a maximum repetition rate of 600 kHz. The helical drilling optics enables the rotation of the incident laser beam through the Dove prism which locates in the hollow shaft motor at a maximum rotational speed of 10,000 rpm. The linear polarized laser beam passes through the spinning Dove prism and rotates with a doubled speed along an optical axis of Dove prism. The incident laser beam is focused to a spot diameter of 15 µm by an objective with a 60 mm effective focal length.

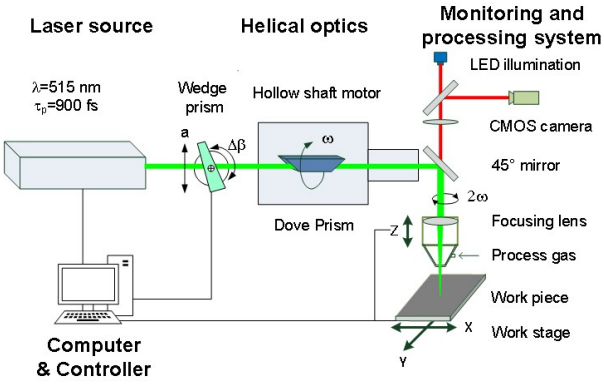

Fig. 1 Schematic of the helical drilling systems

In the helical drilling optics, a wedge prism mounted on a stepper motor changes the inclination angle of laser beam relative to the focusing lens, thus, regulates the helical diameter. In addition, an optical table on a linear stage can shift the laser beam in parallel and alter the inclination angle of focused laser beam relative to workpiece, which generates the taper of holes. The holes are fabricated in 1 mm thick stainless steel X5CrNi18-10.

A multidimensional hole can be fabricated in two steps: firstly, a pilot hole is manufactured via classical helical drilling. Secondly, a shaped inlet with a designated profile is concentrically superposed on the pilot hole using a dynamic helical drilling. Dynamic helical drilling is characterized by a dynamically varied helical diameter and process parameters such as the laser single pulse energy. To characterize the heat affected zone (HAZ) of the pilot hole and shaped inlet, the sample is etched in a V2A-Beize bath for 10 s at a temperature of ca. 70°C. Subsequently, the metallurgical microstructure of the ablated areas are analyzed using a scanning electron microscope (SEM).

The longitudinal cross-section of the fabricated multidimensional holes is prepared so that the drilling depth and hole profile can be observed. Additionally, the surface roughness of shaped section and through pilot hole is measured by a confocal laser scanning microscope (LSM). Moreover, the morphological features of the multidimensional holes are characterized by means of scanning electron microscopy.

3. Results and discussion

3.1 Superposed intensity distribution on helical path

In a classic helical drilling process, where the helical path is constant, the incoming laser pulses are deposited in a sequence on the circular helical path. The position of pulses and the intensity distribution are shown in Fig. 2.

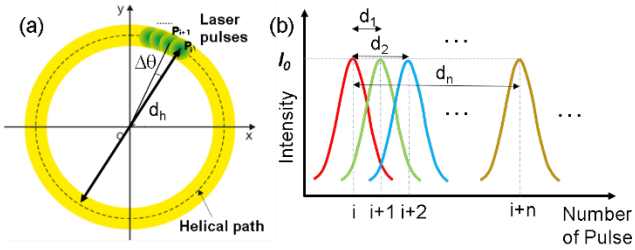

Fig. 2 (a) Overview of the laser pulses train on helical path and (b) the calculation of superposed intensity distribution

The laser pulses has a certain degree overlap with neighboring pulses on the helical path. The angular distance of two neighboring laser pulses Δθ is a matter of pulse density and independent on helical diameter. In the helical drilling process, the angular distance $\Delta\theta$ and between two neighboring laser pulses is given by:

$$\Delta\theta = 2\pi \cdot 2\omega_m \cdot \Delta t = \frac{4\pi\omega_m}{f} \tag{1}$$

As shown in Fig. 2(b) the spatial distance between the i^{th} pulse and the $(i+n)^{th}$ pulse d_n

$$d_n = d_h \sin(n\Delta\theta/2) = d_h \sin(2\pi n\omega_m/f) \tag{2}$$

Here, ω_m is rotation frequency of Dove prism, Δt is the time interval between two consecutive laser pulses, f refers to pulse repetition rate, and d_h is helical diameter.

With the Eqs. (1) and (2), the local superposed laser intensity I_s on focal plane of laser beam is expressed as:

$$I_s = \sum_{i=1}^{ft} I_0 \cdot exp\left(-2\frac{d_{i-1}^2}{\omega_0^2}\right) = \sum_{i=1}^{ft} I_0 \cdot exp\left\{-2\frac{d_h^2 \sin^2[2\pi(i-1)\omega_m/f]}{\omega_0^2}\right\} \tag{3}$$

Where, I_0 is the peak intensity of the laser pulse, ω_0 is the beam intensity 1/e² radius of the laser spot on the focal plane. t refers to the drilling time.

One key parameter in the helical drilling is the local energy deposition which can be described by deposited energy per unit length on the helical path. The overlap degree of laser pulses η_{or} or the number of laser pulses per unit length N_{ppl} can describe the density of laser pulses deposited locally on a single revolution of helical path. They are determined by the spatial distance of pulses and the laser spot size.

By means of the numeric analysis, the superposed intensity distribution with varied helical diameter is plotted and shown in Fig. 3(a). Assuming that the laser parameter, the rotational speed, and focal position are kept constant, the peak intensity drops down dramatically with the increase of helical diameter in a verse-proportional behavior, showing a strong link to the pulse overlap degree. It can also be de-

duced from the Eq. (3) that, $I_s \propto exp(-d_h^2)$. As the helical diameter increases further, the peak of superposed intensity has no significant decrease. Moreover, the single pulse energy, the rotational speed of Dove prism and the laser pulse repetition rate as well as the drilling time play a role in the development of local superposed laser intensity. Fig. 3(b) exhibits the ablation depth by dynamic drilling result. In the process, with constant process parameter, the ablation depth decreases with the increase of helical diameter. The development ablation depth at varied helical diameters is in an excellent agreement with that of superposed laser intensity.as shown in Fig. 3a. The cross-section in Fig.3(c) illustrates the development of ablation depth at greater helical diameter by means of a classic helical drilling. The laser single pulse energy applied is 6.25 µJ and the drilling time is 0.5 s. The helical paths of each diameter are concentric, therefore, the ablated trenches are symmetrically distributed. It reveal again the ablation depth decreases with the increase in the helical diameter.

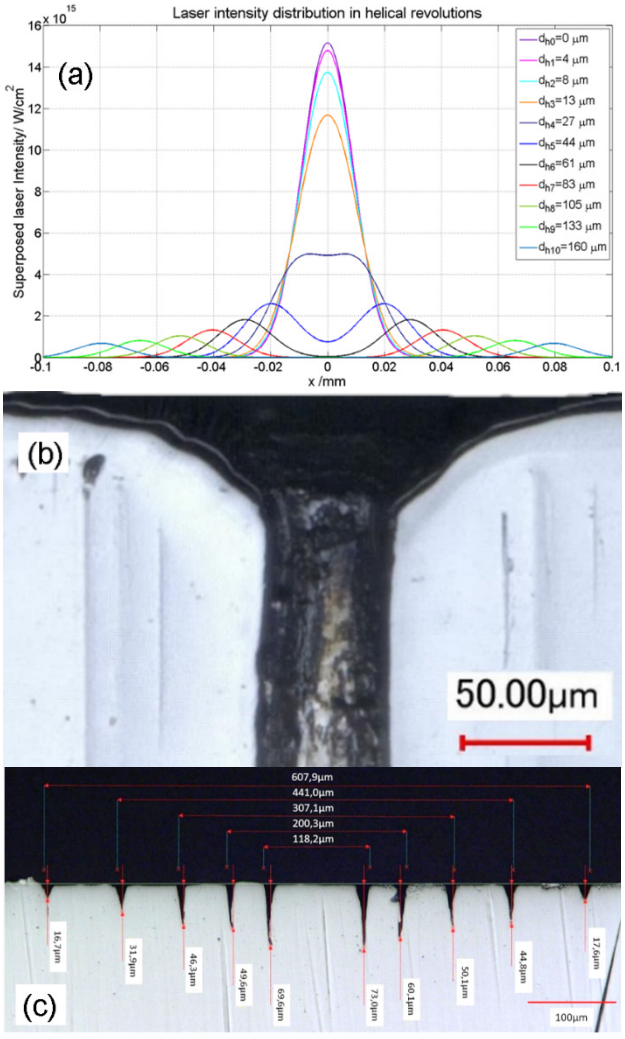

Fig. 3 (a) Diagram of superposed laser intensity on helical revolution , (b) the dynamic ablation results at varied helical diameters and (c) measurement of ablation results at greater helical diameters

As well-known the pulse overlap over the ablation area is constant in the processing using a Galvoscanner, thus, the ablation depth is homogenous. In contrast, the degree of overlap and the ablation depth in the dynamic helical drilling is dependent on the helical diameter. This dependence causes the spatial inhomogeneity of laser energy deposition in the helical drilling and gives the reason why the adaption of energy deposition is possible and necessary for designated hole profile.

3.2 Adaption of energy deposition in dynamic helical process

With regards to the laser energy deposition in helical drilling, the drilling time and single pulse energy have direct link to the local intensity distribution according to the Eq. (3). The influence of drilling time and single pulse energy on the ablation depth at varied helical diameter has been investigated in Fig. 4.

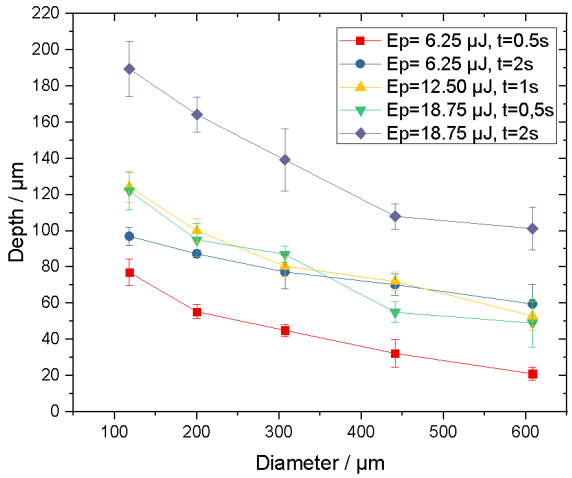

Fig. 4 Diagram of ablation depth in the relationship of helical diameter by varied single pulse energy E_p and drilling time.

With the constant laser pulse energy and repetition rate, the ablation depth at different diameters decreases due to that the deposited energy per unit length decreases. The applied single pulse energy E_p is given in percent value E_p=6.25 µJ, 12.5 µJ and 18.75 µJ. Since the ablation depth of laser pulses depends on the local energy deposition, the parameters of laser beam and helical optics during the helical drilling process must be dynamically adapted in order to achieve a designated profile. It is notable that, the ablation depth is in a quasi-linear relationship with the applied single pulse energy and drilling time if the deviation of measurement is taken into consideration. With the relationship, by varying the pulse energy and pulse density, the deposited energy per unit length on the single helical path can be adapted, thus, the ablation depth can be scaled precisely. To verify the hypothesis, further investigation is conducted with the parameters for adaption of drilling time listed in Tab. 1. The specific value d_h/t is constant at 236.

Table 1 Adaption of drilling time

d_h/µm	Ep/µJ	t/s	f_{REP}/kHz	[d_h/t]
118	12.5	0.500	75	**236**
200	12.5	0.847	75	**236**
307	12.5	1.300	75	**236**
441	12.5	1.860	75	**236**
608	12.5	2.565	75	**236**

With a constant drilling time and applied single pulse energy, the superposed intensity can be also scalable by adapting the spatial distance between two consecutive laser pulses d_l according to Eq. (2). In the helical drilling process, the

component $\omega_m << f$, thus, $d_1 \approx 2\pi d_h \omega_m / f$. If the rotation speed ω_m is kept constant,

$$d_1 \propto d_h / f \tag{4}$$

The parameters for adaption of pulse repetition rate are listed in Tab. 2. Due to the technical condition, the devisor of fundamental frequency must be always an integral, the available pulse repetition rate at each tested helical diameter cannot be given as theoretical calculation. As a result, the component of d_h / f can only be adapted with a minimized deviation.

Table 2 Adaption of pulse repetition rate

d_h/μm	Ep/μJ	t/s	f_{REP}/kHz	$[d_h/f]$
118	12.5	1.33	28.57	**4.1**
200	12.5	1.33	50	**4**
307	12.5	1.33	75	**4.1**
441	12.5	1.33	100	**4.4**
608	12.5	1.33	150	**4**

Fig. 5 shows the ablation behavior with adaption of parameters listed in Tabs. 1 and 2 compared with the ablation development without adaption. The curve of unadapted parameter has the similar tendency as in Fig. 4. The ablation depth drops down with the increase of helical diameter. In contrast to that, the ablation depth keeps constant at approximately 100 μm over the different helical diameter by increasing the drilling time and pulse repetition rate correspondingly. The noticeable deviation of ablation depth can be a combined result of the deviation of the calculated parameter. However, the model matches well with the experimental results and the hypothesis are validated that homogenous ablation is achievable by keeping a constant local superposed laser intensity distribution.

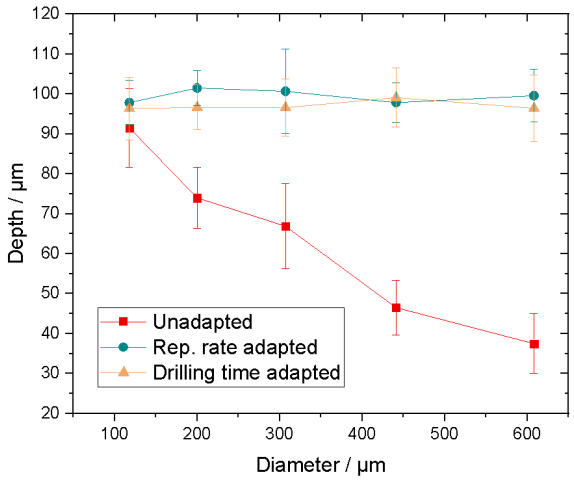

Fig. 5 Ablation depth at varied helical diameter by unadapted process (red square), adapted repetition rate (dark green circle) and drilling time (yellow triangle).

3.3 Fabrication and the characterization of multidimensional hole with adapted energy deposition

With the adapted laser energy deposition, helical drilling with the scalable ablation depth can be performed to fabricate multidimensional microholes with designated profile as the SEM images shown in Fig. 6.

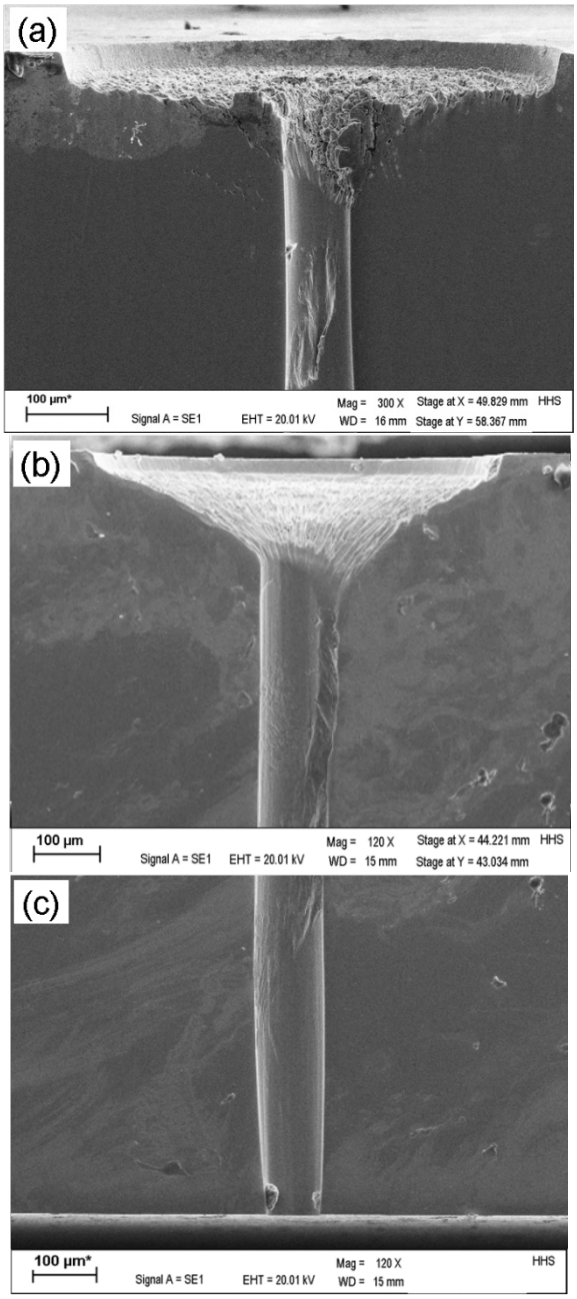

Fig. 6 (a) SEM image of a T-shaped and (b) Y-shaped hole drilled by dynamic helical drilling process, (c) the outlet section of the pilot hole in Y-shaped drilling

The SEM images of cross-section of drilling in Fig. 6 show two examples of multidimensional holes fabricated in stainless steel, i. e. a T-shaped hole and Y-shaped microfunnel. Based on the results and discussion represented in sections 3.1 and 3.2, the applied single pulse energy was adapted in the fabrication of these two shaped holes.

The T-shaped hole in Fig. 6(a) shows an inlet with uniformed depth of about 80 μm and diameter about 600 μm. The single pulse energy applied in this area has been increased from 6.25 μJ near the pilot hole to 18.75 μJ at the outer contour, so that more volume of material can be ablated at larger helical diameter. The microfunnel in Fig. 6(b) exhibits a well-defined frustum profile with a linear slant and a full opening angle of 126 degree. Compared with drilling results with unadapted energy deposition in Fig. 3(b), the Fig. 6(b) demonstrates a linear ablation behavior over the

hole diameter. In more details of the adaption strategy, the increase of applied single pulse energy is a factor of 0.8 of in the T-shaped holes. The surface on the hole inlet has a fish-scale-like morphology and the root mean square roughness Rq=2.43 µm measured by laser scanning microscopy. Whereas the Roughness on the lower pilot hole section at outlet has a Rq < 0.35 µm. The smooth surface of the borehole is visible in Fig. 6(c). The distinction of surface quality of the shaped hole inlet and the lower section of pilot hole is very clear. The shaped inlet is fabricated by a helical ablation process by one to two repeats. The ablation rate is very high to achieve the depth of multiple tens of micron. In addition, the offset of neighboring helical paths at varied diameters is very fine about a couple of hundred nanometers due to the rotational speed of Dove prism. Thus, the vapored material by the laser radiation moves towards the neighboring finished area as a result of the recoil force from the material to be ablated in the following beam revolution. Another possible reason ca be explained as the projection of laser intensity on the tapered ablation front and the reflection of the laser beam on the finished area impairs its surface quality.

Morphological analysis is conducted after the chemical etching process on the shaped inlet as well as the transition part where dynamic helical drilling starts, as shown in Fig. 7. The investigation of the heat-affected zone is to characterize the morphological changes in the surrounding drilling material.

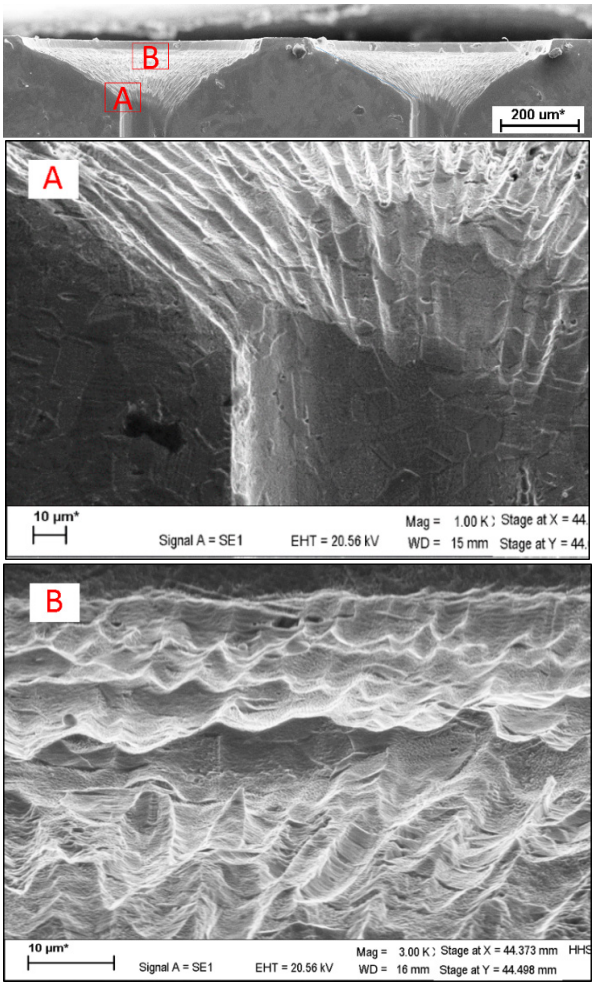

Fig. 7 Metallurgical analysis using SEM on a walls of pilot hole and shaped inlet. The areas A and B are shown in higher magnification for details.

The matrix of the stainless steel used shows the typical features of austenitic chromium-nickel steels in the form of polyhedral grain boundaries and twin boundaries [15]. If the material suffers thermal affect by the heat accumulation, the properties such as grain size and phase of matrix changes. The inspection in Fig. 7 by means of SEM in a magnification of 1000 and 3000 shows the polyhedral grain boundaries and twin boundaries still exist on the ablated surface. It gives evidence that no visible HAZ can be found on the hole wall and shaped inlet as shown in Fig 7(a) and (b). The austenitic grains of the matrix have been precisely cut through by the laser at the transition into the drilling channel. It should be emphasized that the matrix of the drill channels itself can be seen very clearly. Furthermore, no deposits is detectable. Therefore, the dynamic helical drilling process can be characterized as a clean, sublimation-dominated ablation process.

4. Conclusion and outlook

We have presented the strategies for fabrication of multidimensional microholes by means of adapting the local energy deposition during drilling process. The helical drilling process is performed by means of a Dove-prism-based helical optics system and an ultrashort pulsed laser with pulse duration of 900 fs.

The overlap degree of laser pulses deposited on the helical path decreases with the increase of helical diameter. The overlap degree itself has an important influence on the superposed intensity distribution, which reveals the relationship between ablation results and energy deposition. A simple model for helical ablation was built by investigating the development of ablation depth at varied processing parameters. The single pulse energy, the drilling time, the pulse repetition rate and the rotational speed of laser beam are in principle the parameters, which are available for the adaption of energy deposition. Other possible strategies such as adaption of the focal position of laser spot are theoretically feasible as well.

The experimental results are in good agreement with that given by the model. Helical-diameter-independent ablation depth can be achieved by keeping the distance between neighboring pulses $d_i=2\pi d_h\omega_m/f$ or the local superposed laser intensity in terms of single pulse energy and drilling time constant. Depending on the designated hole profile, the energy deposition can be adapted by introducing a factor to achieve a homogenous ablation having high flexibility.

As a final remark, the morphological analysis with SEM on the hole wall show a sublimation-dominated and recast-free ablation process with negligible heat-affected zone by taking advantage of the ultrashort pulsed laser. The matrix and grain size remains on the hole wall after drilling process.

In the future, investigation work to improve the surface quality regarding the surface roughness and homogeneity of the shaped entrance should be done.

Acknowledgments

The authors would like to thank the German Research Foundation DFG for the kind support within the Cluster of Excellence "Internet of Production" - Project-ID: 390621612.

References

[1] L. Romoli, C.A.A. Rashed, and M. Fiaschi: Opt. Laser Technol., 56, (2014) 35.
[2] M. Antar, D. Chantzis, S. Marimuthu, and P. Hayward: Procedia CIRP, 42, (2016) 526.
[3] C. Fohl, D. Breitling, K. Jasper, J. Radtke and F. Dausinger: Proceedings of SPIE, 4426, (2002) 104.
[4] J. Cheng, C. Liu, S. Shang, D. Liu, W. Perrie, G. Dearden, and K. Watkins: Opt. Laser Technol., 46, (2013) 88.
[5] A. Gruner, J. Schille, and U. Loeschner: Physics Procedia, 83, (2016) 157.
[6] H. K. Tönshoff, C. Momma, A. Ostendorf, S. Nolte, and G. Kamlage: J. Laser Appl., 23 (2000) 23.
[7] S. Michel and D. Biermann: Procedia CIRP, 74, (2018) 398.
[8] K. Rahmani-Monfard, A. Fathi, and S. M. Rabiee: Int J Adv Manuf Technol, 84, (2016) 2649.
[9] Z. Liu, B. Wu, A. Samanta, N. Shen, H. Ding, and Y. C. Shin: Manufacturing Letters, 16, (2018) p.18.
[10] M. C. Louwerse, H. V. Jansen, M. N. W. Groenendijk, and M. C. Elwenspoek: J. Micromech. Microeng., 19, (2009) 45008.
[11] S. Michel and D. Biermann: Procedia CIRP, 74, (2018) 398.
[12] T. Beck: Laser Tech. J., 13, (2011) 40.
[13] C. He, J. Bühring, and A. Gillner: Procedia CIRP, 74, (2018) 305.

(Received: May 21, 2019, Accepted: September 5, 2019)

[14] C. He, J. Buehring, F. Zibner and A. Gillner: J. Laser Micro/Nanoeng., 13, (2018) 31.
[15] H.-J. Bargel: "Werkstoffkunde. Mit 85 Tabellen", (Springer, Berlin, 2005).

(Received: May 21, 2019, Accepted: September 5, 2019)